

The LEAP of Pulsars in the Milky Way

M. M. McKinnon

National Radio Astronomy Observatory¹ Socorro, NM, USA

ABSTRACT

The location of objects on the celestial sphere is a fundamental measurement in astronomy, and the distribution of these objects within the Milky Way is important for understanding their evolution as well as the large scale structure of the Galaxy. Here, physical concepts in Galactic astronomy are illustrated using straightforward mathematics and simplifying assumptions regarding the geometry of the Galaxy. Specifically, an analytical model for a smooth distribution of particles in an oblate ellipsoid is used to replicate the observed distributions of the Galactic coordinates for pulsars and supernova remnants. The distributions and the Lambert equal area projections (LEAPs) of the coordinates suggest that the dominant factors determining the general shape of the distributions are the heavy concentration of objects in the Galactic plane and the offset of the Galactic center from the coordinate system origin. The LEAPs and the distributions also show that the dispersion of pulsars about and along the plane are much larger than that for their progenitor supernovae. Additionally, the model can be used to derive an analytical expression for the dispersion measure along any line of sight within the Galaxy. The expression is used to create a hypothetical dispersion measure-distance map for pulsars in the Galaxy.

Subject headings: Pulsars; Supernova remnants; Large scale structure of the Milky Way; Interstellar medium; Globular clusters; Analytical methods

1. Introduction

The distribution of objects in the Milky Way is important for understanding their formation and evolution, as well as the large scale structure of the Galaxy. Although Galactic coordinates are measured with respect to the location of the Sun, most analytical models

¹The National Radio Astronomy Observatory is a facility of the National Science Foundation operated under cooperative agreement by Associated Universities, Inc.

for the locations of objects in the Galaxy use a coordinate system having an origin at the Galactic center (GC; Sartore et al. 2009; Lorimer et al. 2006). And although the locations are measured in a spherical coordinate system, the models are formed using cylindrical coordinates, with the height, azimuth, and equatorial radial distance of the objects taken as independent random variables (RVs). The distribution for azimuth is always uniform over 2π , due to the symmetry provided by a galactocentric origin. The height of an object above the Galactic plane (GP) is almost always treated as an exponential RV (Lorimer et al. 2006; Bahcall 1986; Lyne et al. 1985; Gunn & Ostriker 1970). Most models assume the equatorial radii of stellar coordinates follow gamma or exponential distributions (Lorimer et al. 2006; Bahcall 1986), while others invoke a normal distribution (Sartore et al. 2009). The parameterization of these models requires reasonably accurate estimates of the distances to the objects for a proper transformation of coordinates between the solarcentric and galactocentric coordinate systems. The distance estimates for pulsars (PSRs) are generally made from a model of the distribution of free electrons within the Galaxy (Taylor & Cordes 1993; Cordes & Lazio 2008) in combination with the observed value of a PSR’s dispersion measure. The distance estimates can introduce a significant source of error in the model parameterization because actual measurements of PSR distances via parallax have shown some estimates to be in error by a factor of two or more (Cordes & Lazio 2008; Brisken et al. 2002). The objective of this paper is to develop a solarcentric analytical model of spheroidal Galactic coordinates that can be parameterized without direct knowledge of the distances to objects in the Galaxy.

The distribution of objects within the Galaxy is perhaps best illustrated by a Lambert equal area projection (LEAP), which is a polar plot of the Galactic coordinates of the objects in the two hemispheres of the celestial sphere (e.g. see Figs. 1 and 2). The main advantage of a LEAP is it preserves the density of data points in the projection, unlike other projection methods (e.g. orthographic) which do not (Fisher et al. 1987). A LEAP consists of two sets of concentric circles centered on the location of the Sun. The left set of circles in a LEAP is the projection as viewed from above the GP, and the right set is the view from below the GP. The azimuth and radius of the points in the polar plots represent an object’s Galactic coordinates. Galactic longitude, ϕ , is equal to a point’s azimuth in a LEAP and increases in the counterclockwise direction from the GC, which is located at the far right of each circle set. A point’s radius in the polar plot is equal to $2 \sin(\theta/2)$, where θ is the Galactic colatitude of the object. Objects located in the GP fall on the perimeter of the LEAP, and those located off the GP reside within the perimeter.

The LEAPs of PSRs and supernova remnants (SNRs) are shown in Figures 1 and Figure 2, respectively. Since PSRs are born in supernovae, one might expect their distributions on the sky to be similar. Both objects reside primarily in the GP in what is known as a

girdle-type distribution in the statistical literature (Fisher et al. 1987). The LEAPs show the dispersion of PSRs perpendicular to the GP is much greater than that of their progenitor SNRs. The same may also be true of the dispersion along the GP.

2. Statistical Model of Galactic Coordinates

An analytical, statistical model was developed to derive a joint probability density for the Galactic coordinates of any type of object (e.g. PSR, SNR, star, HII region, globular cluster, etc.) in the Galaxy. The motivation for developing the model is to quantify and explore the differences in the spatial distributions of PSRs and SNRs.

The model’s coordinate system has an origin corresponding to the location of the Sun. Its x-axis lies in the direction of the GC, and its z-axis is perpendicular to the GP. The model assumes the Cartesian coordinates of the objects are independent, normal RVs. The assumption of normal RVs allows an analytical solution to be derived because the coordinate distributions are continuous at all locations within the model galaxy. The RV representing the z-coordinate has a zero mean and a standard deviation $\sigma_z = \sigma$, which is the dispersion of the objects *about* the GP. The RV representing the x-coordinate has a mean equal to the distance, R_o , between the Sun and the GC and a standard deviation of $\sigma_x = \sigma(1 + \rho^2)^{1/2}$, which is the dispersion of the objects *along* the GP. The RV for the y-coordinate has a zero mean and a standard deviation equal to σ_x . By construction, the model inherently assumes the Sun resides precisely in the GP. As with most other analytical models of the Galaxy, the model neglects the structure of the Galaxy’s spiral arms.

The model imposes the form of an oblate ellipsoid on the three-dimensional distribution of objects in the Galaxy. The ellipsoid is centered on the GC and has an axial ratio equal to $(1 + \rho^2)^{1/2}$. The model produces a smooth, yet continuously varying, spatial density of objects in the Galaxy. An analytical expression for the density, n , as a function of distance, r , longitude, and colatitude can be computed from the model assumptions by multiplying the probability densities for the x, y, and z coordinates by one another, since they are independent RVs, and converting these Cartesian coordinates to spherical ones. The density is

$$\begin{aligned}
 n(r, \theta, \phi) &= \frac{1}{\sigma^3(1 + \rho^2)(2\pi)^{3/2}} \exp \left[\frac{-R_o^2(1 + \rho^2 \cos^2 \theta - \sin^2 \theta \cos^2 \phi)}{2\sigma^2(1 + \rho^2)(1 + \rho^2 \cos^2 \theta)} \right] \\
 &\times \exp \left\{ \frac{-(1 + \rho^2 \cos^2 \theta)}{2\sigma^2(1 + \rho^2)} \left[r - \frac{R_o \sin \theta \cos \phi}{(1 + \rho^2 \cos^2 \theta)} \right]^2 \right\}.
 \end{aligned} \tag{1}$$

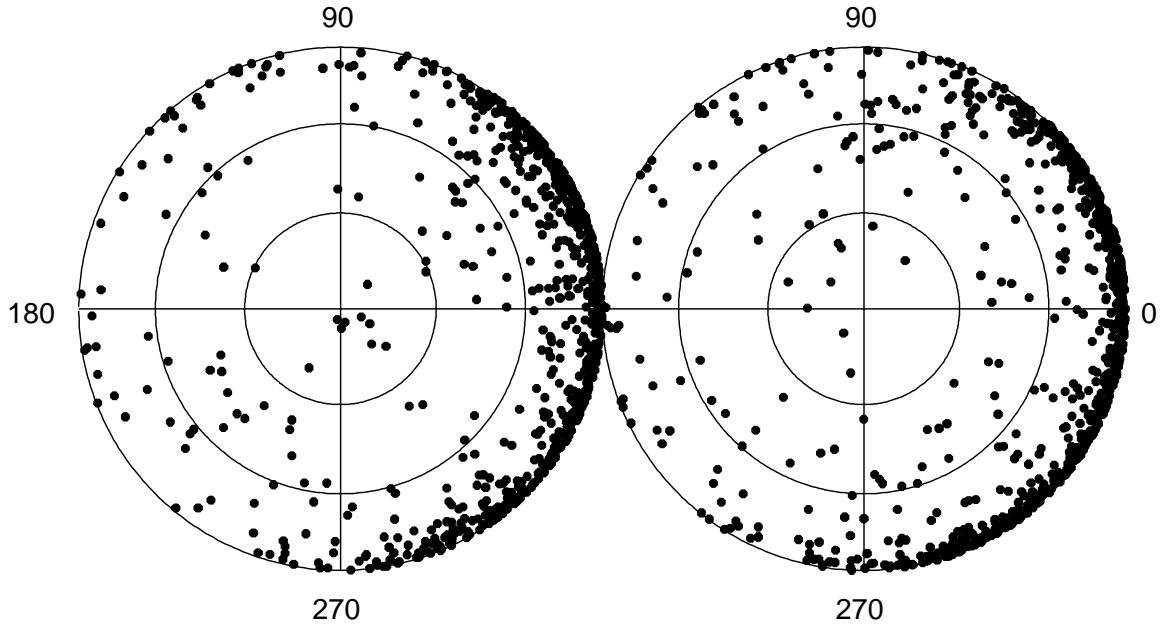


Fig. 1.— Lambert equal-area projection of pulsar Galactic coordinates. The perimeter of the figure corresponds to the Galactic plane. The concentric circles are lines of constant Galactic colatitude.

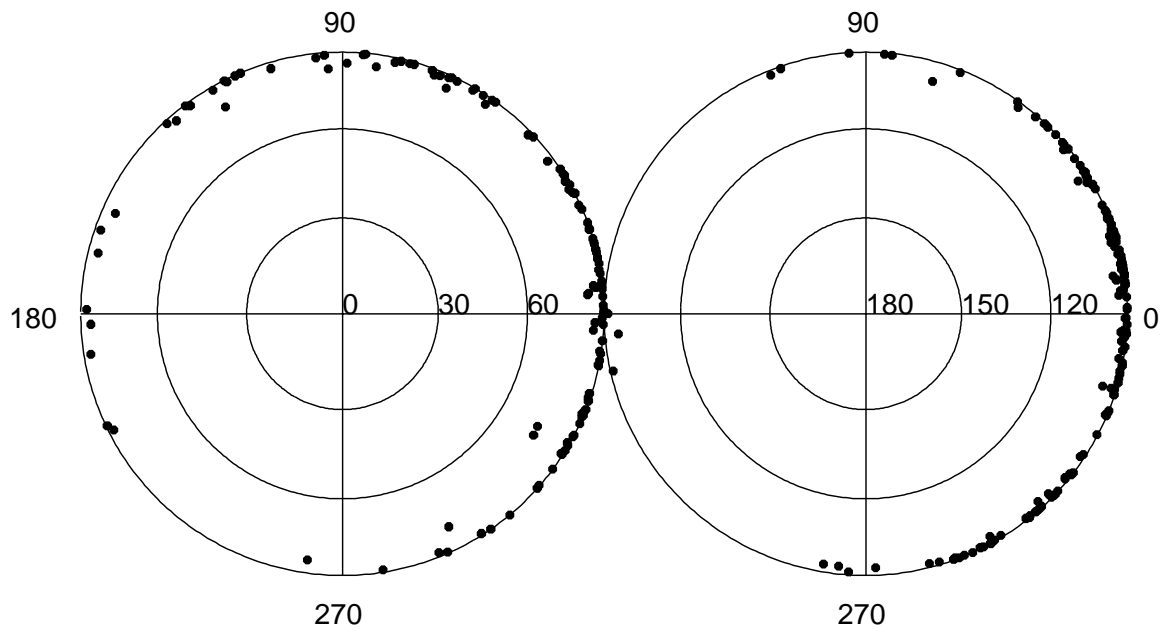


Fig. 2.— Lambert equal-area projection of supernova Galactic coordinates. The numbers on the perimeter of the figure denote Galactic longitude. The numbers labelling the interior concentric circles denote Galactic colatitude.

As written, the equation for density is normalized such that it integrates to unity over volume. The actual number density is the density multiplied by a constant equal to the total number of objects in the Galaxy.

2.1. Joint Probability Density of Galactic Coordinates

The joint probability density of an object’s Galactic colatitude and longitude can be calculated by integrating the density over radius. The joint probability density is

$$\begin{aligned} f(\theta, \phi) &= \sin \theta \int_0^\infty n(r, \theta, \phi) r^2 dr \\ &= u \exp \left[-\frac{s^2}{2(1+\rho^2)} \right] \left\{ \exp \left(\frac{v^2}{2} \right) \left[1 + \operatorname{erf} \left(\frac{v}{\sqrt{2}} \right) \right] (1+v^2) + v \sqrt{\frac{2}{\pi}} \right\}, \end{aligned} \quad (2)$$

where $\operatorname{erf}(x)$ is the error function, and u and v are functions of θ and ϕ given by

$$u(\theta) = \frac{\sin \theta}{4\pi} \frac{(1+\rho^2)^{1/2}}{(1+\rho^2 \cos^2 \theta)^{3/2}} \quad (3)$$

$$v(\theta, \phi) = \frac{s \sin \theta \cos \phi}{[(1+\rho^2)(1+\rho^2 \cos^2 \theta)]^{1/2}} \quad (4)$$

The joint density is a function of two free parameters, $s = R_o/\sigma$ and ρ . The inverse of the parameter s , in units of radians, is the angular dispersion of the objects in Galactic colatitude. The quantity $(1+\rho^2)^{1/2}/s$, again in units of radians, is related to the angular dispersion in Galactic longitude. The colatitude distribution narrows with increasing s . The longitude distribution narrows with increasing s and decreasing ρ . A fit of the distribution of an object’s coordinates to Equation 2 does not require distance information because distance was eliminated in the calculation of the angles’ joint probability density with the integration over r .

2.2. Pulsar Dispersion Measure

The dispersion measure (DM) of a PSR is the density of free electrons in the interstellar medium integrated over the distance, d , to the PSR. The model developed here specifies the position-dependent density of any object in the Galaxy. One can compute an analytical expression for DM along any line of sight by assuming the objects in the model are free electrons. The DM is

$$\begin{aligned}
\text{DM}(d, \theta, \phi) &= N_e \int_0^d n(r, \theta, \phi) dr \\
&= \frac{N_e}{4\pi\sigma^2} \frac{\sqrt{2}}{g(\theta)} \exp \left[-\frac{R_o^2(1 + \rho^2 \cos^2 \theta - \sin^2 \theta \cos^2 \phi)}{\sigma^2 g^2(\theta)} \right] \\
&\times \left\{ \text{erf} \left[\frac{d(1 + \rho^2 \cos^2 \theta) - R_o \sin \theta \cos \phi}{\sigma g(\theta)} \right] + \text{erf} \left[\frac{R_o \sin \theta \cos \phi}{\sigma g(\theta)} \right] \right\}, \quad (5)
\end{aligned}$$

where N_e is the total number of free electrons in the Galaxy, and $g(\theta)$ is a function of Galactic colatitude given by

$$g(\theta) = [2(1 + \rho^2)(1 + \rho^2 \cos^2 \theta)]^{1/2}. \quad (6)$$

3. Data Analysis

Two-dimensional histograms of the colatitude and longitude for PSRs and SNRs were computed using coordinates given in the ATNF PSR catalog (Manchester et al. 2005) and Green’s (2004) catalog of Galactic SNRs. The PSR data were edited to exclude extragalactic PSRs and multiple PSRs in globular clusters. Estimates of s and ρ were made with a two-dimensional, least squares fit of the histograms to the joint probability density given by Equation 2.

The results of the fit are shown in Table 1 and Figure 3. The entries in the table are the number of objects in each fit, N , the fit parameters, s and ρ , the axial ratio of each object’s oblate ellipsoid, $(1 + \rho^2)^{1/2}$, and the dispersions perpendicular and parallel to the GP as calculated from s and ρ assuming $R_o = 8.5$ kpc. Figure 3 shows histograms of colatitude and longitude computed from the PSR and SNR catalog data. Theoretical distributions of θ and ϕ were calculated by numerically integrating the joint density over ϕ and θ , respectively, using the values of s and ρ obtained from the least squares fits. The continuous solid line in each panel of the figure shows the fitted theoretical distribution.

To explore the verstatility of the model, the same analysis was applied to the Galactic coordinates for globular clusters using data from the catalog maintained by Harris (1996). The results of the analysis are summarized in the last row of Table 1. The LEAP and coordinate histograms for globular clusters are not shown.

Equation 5 was used to develop a hypothetical DM-distance map for PSRs in the Galaxy (Fig. 4). The rather arbitrary parameters used to produce the map were $R_o = 8.5$ kpc, $\sigma = 0.4$ kpc, $\rho = 20$, and $N_e/\sigma^2 = 9 \times 10^4$ pc/cm³. A physical boundary for the Galaxy had to be estimated to produce the map. The boundary is the edge of the Galaxy, or maximum

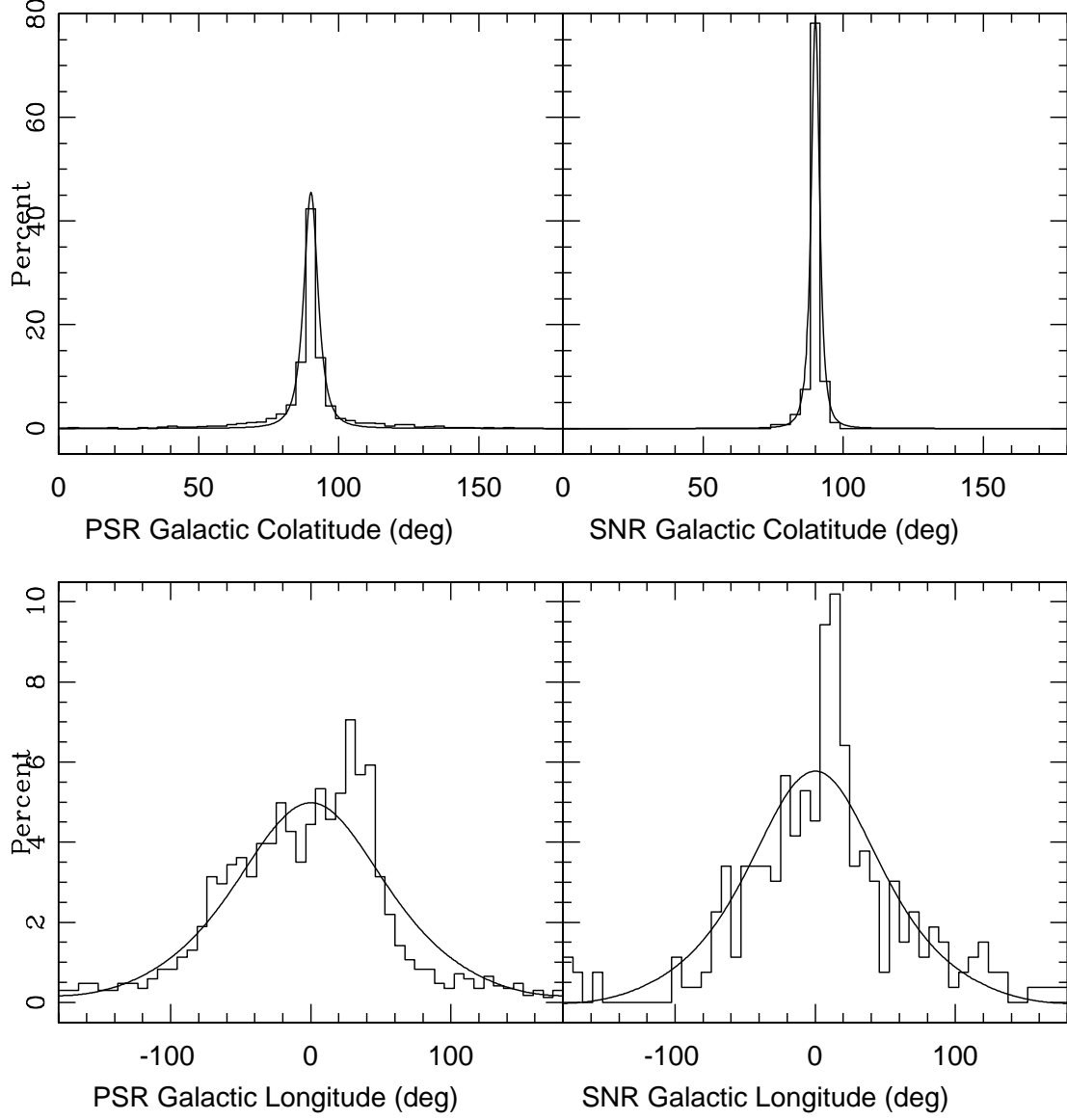


Fig. 3.— Histograms of the Galactic colatitude (top panel) and longitude (bottom panel) for pulsars and supernova remnants. The histograms were computed from the measured coordinates of the objects. The continuous solid line in each panel denotes the best fit of Equation 2 to the two-dimensional histogram of each object's coordinates.

distance, r_{max} , along any line of sight. It was estimated from the equation for the surface of an ellipsoid with the maximum extent of the Galaxy taken to be 3σ from the GC in the z-direction and $3\sigma(1+\rho^2)^{1/2}$ from the GC in the x- and y-directions. The maximum distance is

$$r_{max}(\theta, \phi) = \frac{R_o \sin \theta \cos \phi + \{R_o^2 \sin^2 \theta \cos^2 \phi + [9\sigma^2(1 + \rho^2) - R_o^2][\sin^2 \theta + (1 + \rho^2) \cos^2 \theta]\}^{1/2}}{\sin^2 \theta + (1 + \rho^2) \cos^2 \theta}. \quad (7)$$

The solid lines in the figure show the Galactic boundary in DM-distance space. Ideally, all values of DM and distance for PSRs in the Galaxy would reside within this boundary. The upper boundary gives the maximum DM as a function of distance for PSRs residing in the direction of the GC. It terminates at the far side of the Galaxy on the right side of the figure. The lower right boundary of the map is the DM measured at the edge of the Galaxy for lines of sight within the GP having different values of longitude. (When $\theta = \pi/2$, the lower boundary in the map is the same for longitudes in the range $0 \leq \phi \leq \pi$ as it is for the longitudes $2\pi \geq \phi \geq \pi$ due to the geometric symmetry of the problem). The cusp in the boundary at a distance of about 17 kpc occurs at the Galactic anti-center. The lower left boundary in the map is the DM-distance relation for lines of sight with longitude fixed at $\phi = \pi$ and colatitude varying in the range $0 \leq \theta \leq \pi/2$. The cusp near $d \simeq 1$ kpc is the maximum DM at the edge of the Galaxy directly above and below the Sun. The small boundary spur in the range $0 < d \leq 1$ kpc is the DM measured between the Sun and the edge of the Galaxy above and below it. The dotted lines in the map show how the DM varies with distance for lines of sight within the GP having fixed values of longitude. The dashed line is the maximum DM as a function of distance when the longitude of the line of sight is fixed at $\phi = 0$ with the colatitude varying between 0 and $\pi/2$.

Table 1. Derived Parameters for the Joint Probability Density of Galactic Coordinates for Pulsars, Supernova Remnants, and Globular Clusters

Object	N	s	ρ	$(1 + \rho^2)^{1/2}$	σ_z (kpc)	σ_x (kpc)
Pulsars	1687	10.4	12.7	12.8	0.8	10.4
Supernova Remnants	265	21.8	19.2	19.2	0.4	7.5
Globular Clusters	150	3.8	0.6	1.2	2.2	2.6

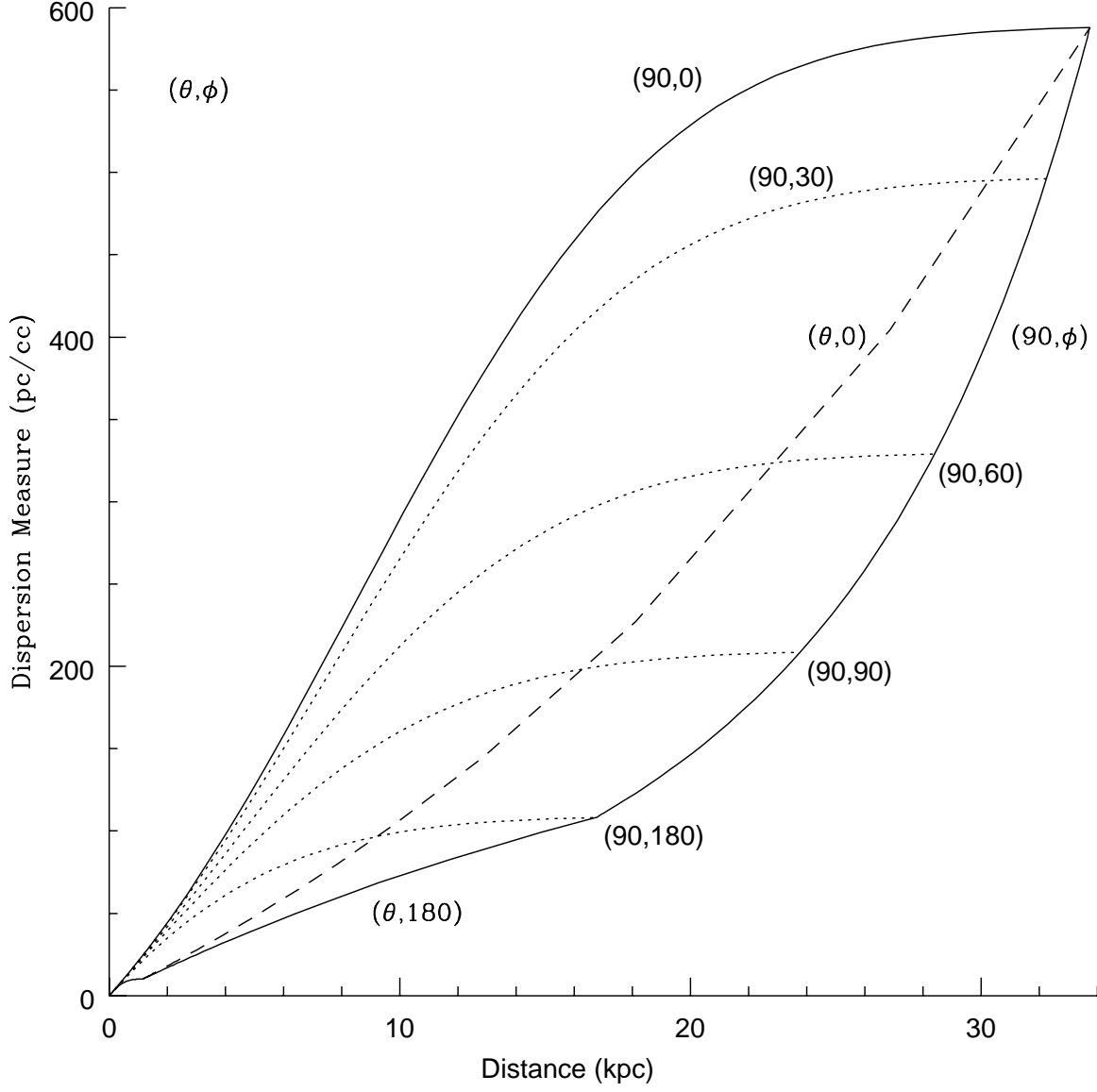


Fig. 4.— Hypothetical dispersion measure-distance map for pulsars in the Galaxy. The numbers in parenthesis denote the colatitude, θ , and longitude, ϕ , in units of degrees, for different lines of sight through the Galaxy.

4. Results and Discussion

The angular dispersion of colatitude can be calculated from the inverse of the value of s obtained in the model fit. From the entries in Table 1, the calculation gives an angular dispersion in colatitude of about 5.5 degrees for PSRs and about 2.6 degrees for SNRs. The angular dispersion in longitude can be calculated from the fit values of s and ρ . The dispersion in longitude for PSRs and SNRs is 71 degrees and 50 degrees, respectively. Summarizing the fit results for PSRs by stating them another way, most observed PSRs reside within Galactic longitudes of ± 71 degrees and within Galactic latitudes of ± 5.5 degrees.

The entries in Table 1 indicate that the three dimensional spatial distributions of PSRs and SNRs are consistent with oblate ellipsoids. The PSR ellipsoid has an axial ratio of about 13, while the SNR axial ratio is about 19. A representation of the “one-sigma” contours of the distributions of PSRs and SNRs in the Galaxy is drawn to scale in Figure 5. The two dots represent the locations of the GC and the Sun. Their separation of $R_o = 8.5$ kpc sets the scale for the figure. The figure shows that the Sun resides on the edge of the SNR contour.

The entries in Table 1 show the dispersion of PSRs perpendicular to the GP is about a factor of two larger than that for SNRs. The difference is likely caused by the kick velocity acquired by the PSR in the explosion of its progenitor supernova (Gunn & Ostriker 1970). The kick accounts for the high proper motions of PSRs and their locations outside the GP. The dispersion of PSRs along the GP is about 40% larger than that for SNRs. It may be caused by a component of PSR kick velocity along the GP.

The analysis presented here likely underestimates the actual value of s and overestimates the actual value of ρ for PSRs. Searches for PSRs rely on the impulsive nature of PSRs for their detection. Multipath scattering in the interstellar medium can significantly broaden the pulse, making them more difficult to find, particularly towards the GC where the scattering can be severe. Consequently, PSRs are undersampled towards the GC and the actual distribution of PSRs is more heavily populated at $\theta = \pi/2$ and $\phi = 0$ than what is shown in Figure 3. This selection effect causes the fitted value of s to be smaller than its actual value and the fitted value of ρ to be larger. Thus, the calculated value of σ_z should be regarded as an upper limit since it varies inversely with s and the actual value of s is likely larger than the fitted one. By a similar argument, the fitted value of σ_x should also be regarded as an upper limit.

The results obtained by fitting observed coordinates to the model are reasonably consistent with those produced from other models of the Galaxy. The major components comprising the large scale structure of the Galaxy include, at a minimum, a spheroid of old stars and globular clusters and a thin disk of younger stars and atomic and molecular gas

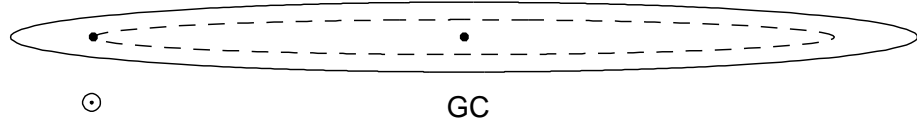


Fig. 5.— $1 - \sigma$ contours for the distribution of pulsars (solid line) and supernova remnants (dashed line) within the Galaxy. The contours are drawn to scale.

(Bahcall 1986; Cox 2000). The Galaxy may contain other components, such as a “thick” disk, a central bulge, and a halo of unseen stars. For the spheroid, Bahcall (1986) lists an effective radius of 2.7 kpc and a major-to-minor axial ratio of about 1.25. When applied to globular clusters, the model described in this paper gives a spheroid effective radius in the range of 2.2 to 2.6 kpc and a spheroid axial ratio of 1.2. For the disk, Bahcall gives an exponential scale height of 0.3 kpc. Here, the dispersion in SNRs about the GP is estimated at 0.4 kpc. The estimate of 0.8 kpc for the dispersion of PSRs about the GP may be more consistent with the scale height (1.3 kpc) Bahcall lists for a thick disk.

In principle, those PSRs having accurate DM and distance measurements (Briskin et al. 2002; Chatterjee et al. 2009) could be used to calibrate the model for the distribution of free electrons in the Galaxy by a non-linear least squares fit of the data to Equation 5. The fit was made, but the resulting values of χ^2 did not decrease as more measurements were included in the fit. This means Equation 1 is not the most accurate representation of the electron density, which is not surprising since we know the distribution of electrons in the Galaxy is not smooth and is heavily influenced by the presence of the spiral arms (Cordes & Lazio 2008). Nonetheless, the DM relationship (Eqn. 5) is useful for a conceptual illustration of how DM might vary with different views through the Galaxy (e.g. Fig. 4).

The model presented here could be extended to other astrophysical problems, such as the emission measure (EM) along different lines of sight within the Galaxy, DM variations in globular clusters, and column density measurements of proto-stellar cores. The EM can be easily calculated by squaring the electron density given by Equation 5 and integrating the result over distance. Multiple PSRs have been discovered in globular clusters (Ransom et al. 2005; Freire et al. 2003), and it may be possible to probe the electron density profile of a cluster with this model if the differences in the DMs and angular separations of the PSRs in the cluster are measureable. Only minor revisions to the model would be required, such as compensating the model coordinate system for the location of the globular cluster and approximating the cluster geometry as a sphere (i.e. by setting $\rho = 0$). The column density of a proto-stellar core is the density integrated over a specific line of sight through the entire core (Dapp et al. 2009). The calculation of column density is very similar to the calculation of maximum DM presented in this analysis. As with the globular cluster analysis, the model would need to be revised slightly to accommodate the viewing geometry of the core. One could incorporate different density profiles in the model and evaluate them in a comparison with the column density measurements.

5. Conclusions

An analytical model with a solarcentric, spherical coordinate system was developed for the distribution of objects in the Galaxy in an attempt to circumvent complications introduced by the galactocentric, cylindrical coordinate system used in other models. Unlike these previous models, the present model does not require distance estimates for its parameterization. The model reasonably describes histograms of measured coordinates for PSRs and SNRs and was used to quantify the differences in their distribution parameters. The dispersion of PSRs perpendicular to and along the GP is larger than that for SNRs. The difference is likely caused by the kick velocity acquired by a PSR in the explosion of its progenitor SNR. SNRs reside in a thin disk of the Galaxy, while PSRs are located in a thicker disk. When applied to globular clusters, the model shows the clusters reside in a spheroid centered on the GC. The model can be applied to other objects to quantify their spatial distribution and perhaps the large scale structure of the Galaxy.

REFERENCES

- Bahcall, J. N., 1986, ARAA, 24, 577
- Briskin, W. F., et al., 2002, ApJ, 571, 906
- Chatterjee, S., et al., 2009, ApJ, 698, 250
- Cordes, J. M. & Lazio, T. J. W., 2008, astro-ph/0207156v3
- Cox, A., 2000, Allen’s Astrophysical Quantities, (New York: Springer)
- Dapp, W. B. & Basu, S., 2009, MNRAS, 395, 1092
- Fisher, N. I, Lewis, T., & Embleton, B. J. J., 1987, Statistical Analysis of Spherical Data, (Cambridge: Cambridge)
- Freire, P. C., et al., 2003, MNRAS, 340, 1359
- Green, D. A., 2004, A Catalogue of Galactic Supernova Remnants, www.mrao.cam.ac.uk/surveys/snrs/
- Gunn, J. E. & Ostriker, J. P., 1970, ApJ, 160, 979
- Harris, W. E., 1996, AJ, 112, 1487 www.physics.mcmaster.ca/resources/globular.html
- Lorimer, D. R. et al., 2006, MNRAS, 372, 777
- Lyne, A. G., Manchester, R. N., & Taylor, J. H., 1985, MNRAS, 213, 613
- Manchester, R. N. et al., 2005, AJ, 129, 1993, www.atnf.csiro.au/research/pulsar/psrcat
- Ransom, S. M., et al., 2005, Science, 307, 892

Sartore, N., et al., 2009, astro-ph/0908.3182v1

Taylor, J. H. & Cordes, J. M. 1993, ApJ, 411, 674